Supplementary Material

Opposite mass balance variations between glaciers in western Tibet and the western Tien Shan

Meilin Zhu[a,c,*], Tandong Yao[b], Shengqiang Jin[b], Wei Yang[b], Yang Xiang[d], Lonnie G. Thompson[c], Huabiao Zhao[b,e,*]

[a] Center for the Pan-Third Pole Environment, Lanzhou University, Lanzhou 730000, China

[b] Key Laboratory of Tibetan Environment Changes and Land Surface Processes, Institute of Tibetan Plateau Research, Chinese Academy of Sciences (CAS), Beijing 100101, China

[c] Byrd Polar and Climate Research Center, The Ohio State University, Columbus, OH 43210, USA

[d] College of Geomatics, Xi'an University of Science and Technology, Xi'an 710054, Shaanxi, China

[e] Ngari Station for Desert Environment Observation and Research, Institute of Tibetan Plateau Research, CAS, Tibet, China

Corresponding author:

E-mail address: zhuml517@163.com (M. Zhu) and zhaohb@itpcas.ac.cn (H. Zhao)

Contents of this file

Figures S1 to S7

Figures

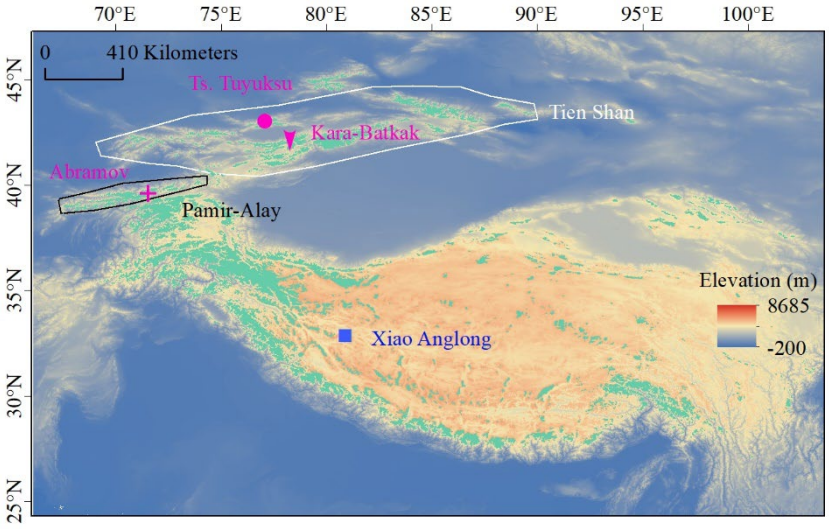

Figure S1 Geographical locations of the study area and selected glaciers. White and black polygons indicate the Tien Shan and Pamir-Alay, respectively. Blue and pink polygons indicate the selected regions of western Tibet and the western Tien Shan, respectively. Symbols are as follows: pink dot, Ts. Tuyuksu Glacier; pink inverted triangle, Kara-Batkak Glacier; pink cross, Abramov Glacier; blue square, Xiao Anglong Glacier. Glaciers are marked by a jade color.

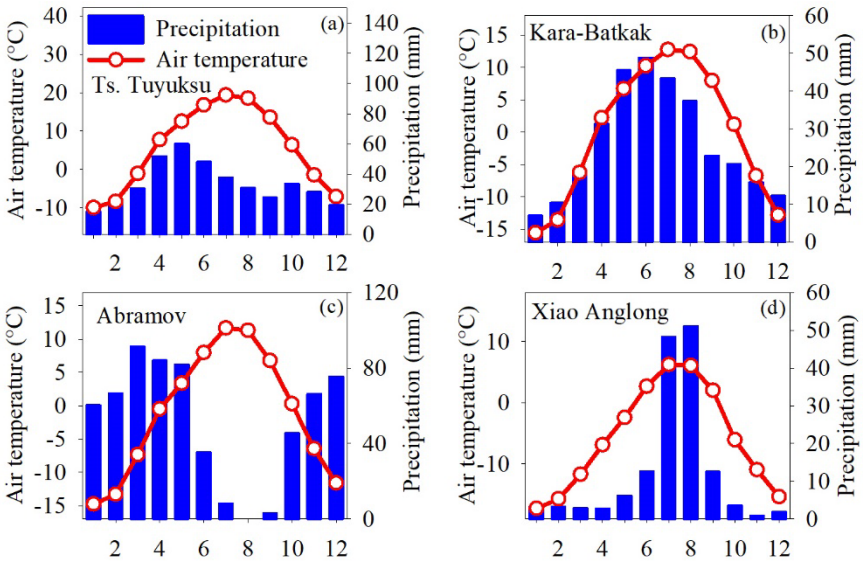

Figure S2 Mean monthly precipitation and air temperature for (a) Ts. Tuyuksu, (b) Kara-Batkak, (c) Abramov, and (d) Xiao Anglong glaciers during 1970-2019. The data for Ts. Tuyuksu, Kara-Batkak, and Abramov glaciers are from CRU; the altitudes (latitudes and longitudes) of grid points for Ts. Tuyuksu, Kara-Batkak, and Abramov glaciers are 1984 m (43.25°N and 77.25°E), 2954 m (42.25°N and 78.25°E) and 3478 m (39.75°N and 71.75°E), respectively. The data for Xiao Anglong Glacier are the reconstructed values at AWS site from Zhu et al. (2021b). AWS was established at 5141 m (32.91°N and 81.42°E), approximately 7.5 km northeast of Xiao Anglong Glacier.

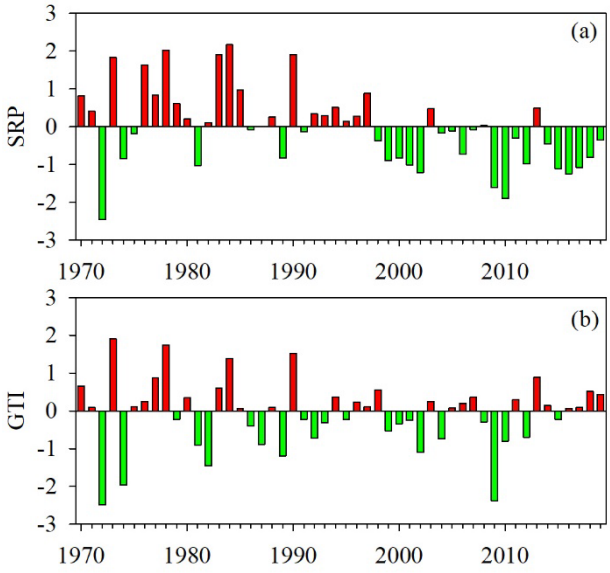

42

43 **Figure S3** The Silk Road Pattern (SRP) index (a) and global wave train index (GTI) (b) for the

44 ablation season from 1970 to 2019.

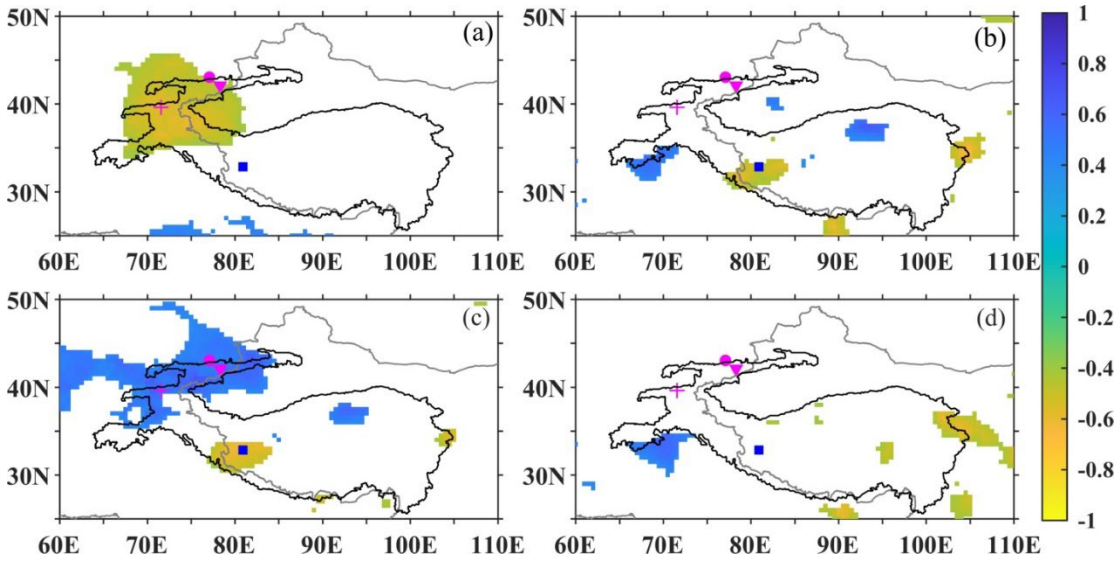

Figure S4 Spatial distribution of linear correlation coefficients from 1970 to 2019 using correlation analysis between detrended ablation season mass balance on Kara-Batkak Glacier and (a) detrended CRU gridded ablation season air temperature data, (b) detrended CRU gridded annual precipitation data, (c) detrended CRU gridded ablation season precipitation data, and (d) detrended CRU gridded cold season precipitation data. Only significant correlations ($p < 0.05$) are shown on all figures. Symbols are as follows: pink dot, Ts. Tuyuksu Glacier; pink inverted triangle, Kara-Batkak Glacier; pink cross, Abramov Glacier; blue square, Xiao Anglong Glacier.

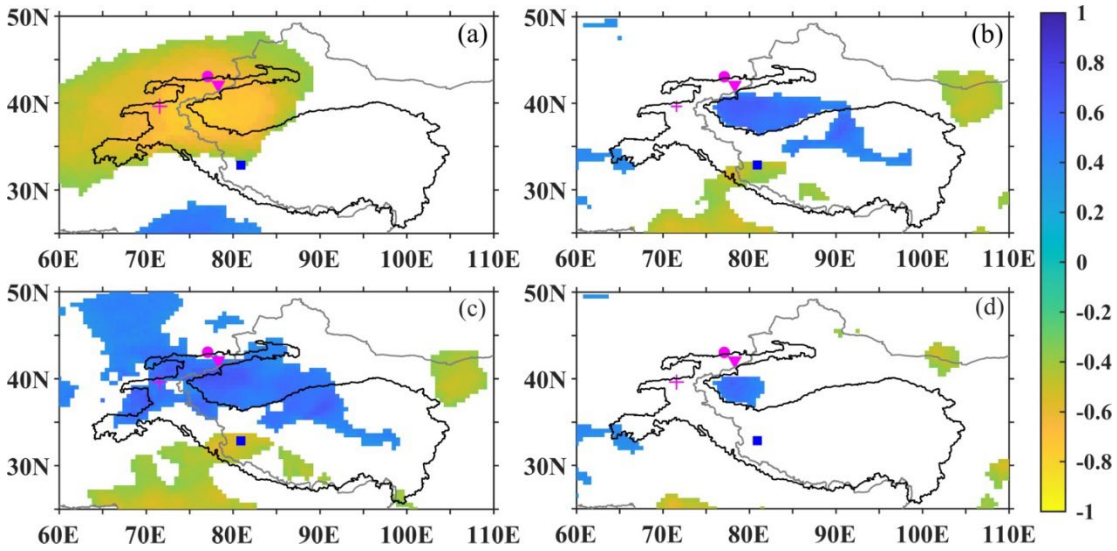

Figure S5 Spatial distribution of linear correlation coefficients from 1970 to 2019 using correlation analysis between detrended ablation season mass balance on Abramov Glacier and (a) detrended CRU gridded ablation season air temperature data, (b) detrended CRU gridded annual precipitation data, (c) detrended CRU gridded ablation season precipitation data, and (d) detrended CRU gridded cold season precipitation data. Only significant correlations ($p < 0.05$) are shown on all figures. Symbols are as follows: pink dot, Ts. Tuyuksu Glacier; pink inverted triangle, Kara-Batkak Glacier; pink cross, Abramov Glacier; blue square, Xiao Anglong Glacier.

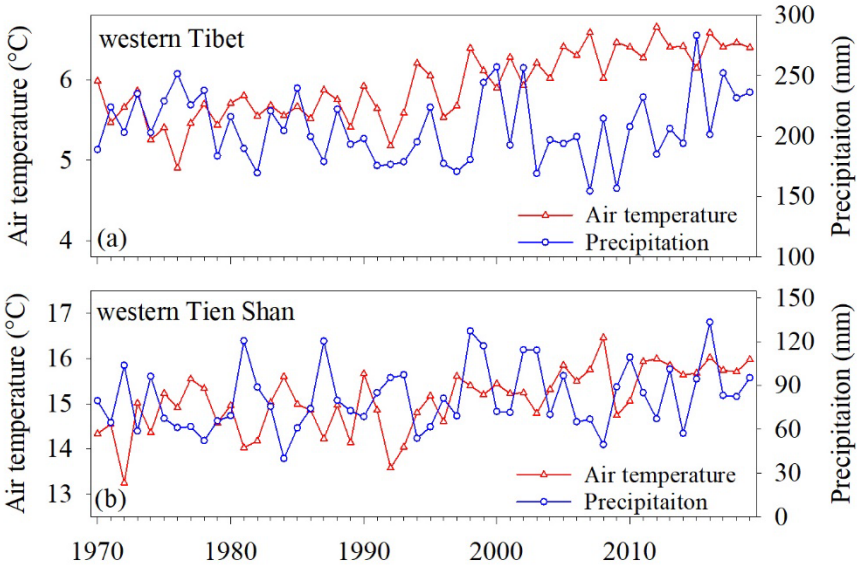

Figure S6 Regionally averaged ablation season air temperature (T_a) and precipitation in (a) western Tibet (30.5–34.5°N, 80–85°E) and (b) the western Tien Shan (39.25–43.25°N, 71.25–79.25°E).

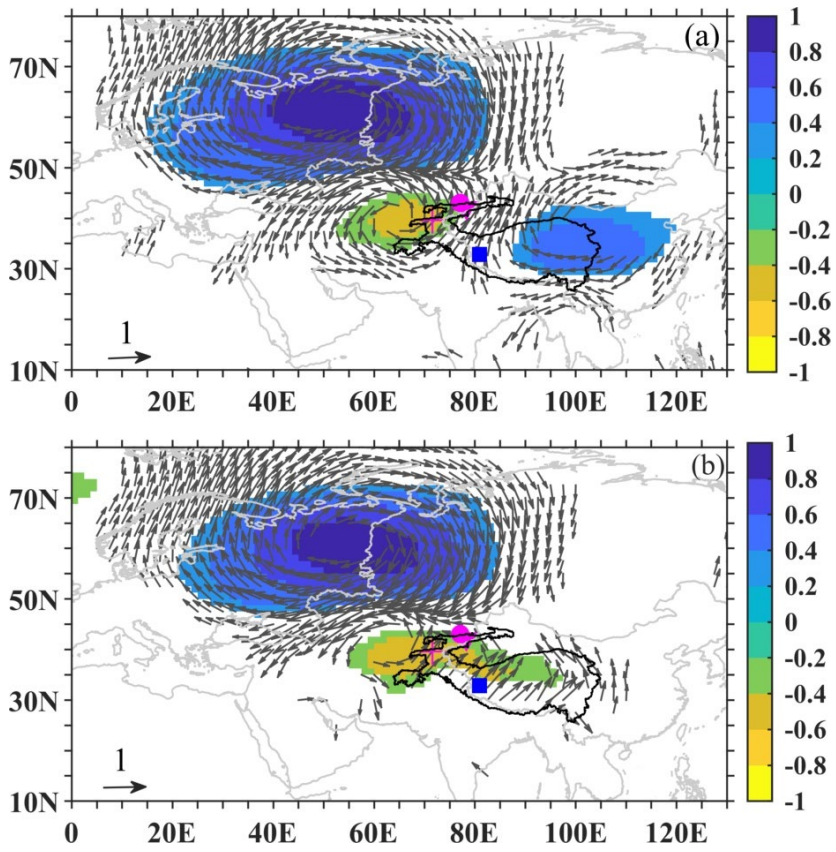

Figure S7 The correlation analysis of the 300 hPa regionally-averaged geopotential height over Europe (55°–68°N, 35°E–70°E) with (a) 300 hPa, and (b) 600 hPa geopotential height (gpm)/wind fields during the ablation season from 1970 to 2019. All data are detrended. Only significant correlations ($p < 0.05$) are shown. Vectors are composites of the correlations with horizontal wind components (zonal and meridional wind speed): a significant vector denotes either one of its components is significant. The geopotential height and wind fields are from the JRA55 dataset. Symbols are as follows: pink dot, Ts. Tuyuksu Glacier; pink inverted triangle, Kara-Batkak Glacier; pink cross, Abramov Glacier; blue square, Xiao Anglong Glacier.

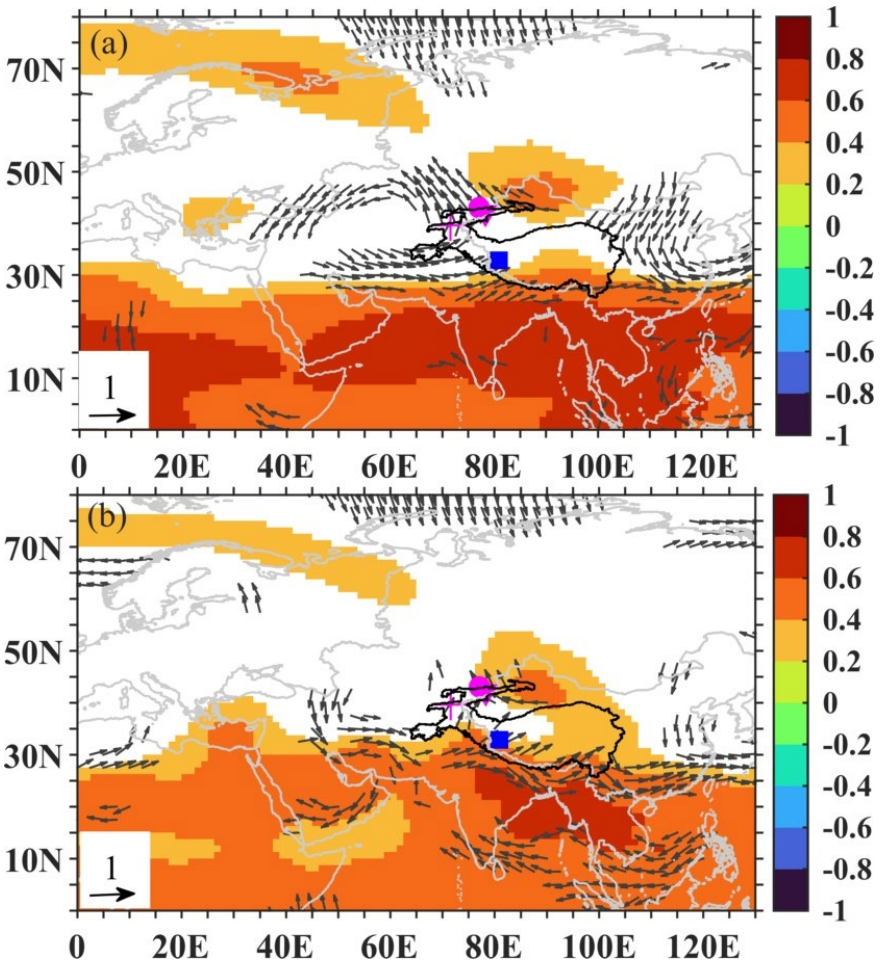

Figure S8 Spatial correlations of regionally averaged sea surface temperature over the northern Arabian Sea (15.5°–23.5°N, 60°E–70°E) with (a) 300 hPa and (b) 600 hPa geopotential height (gpm)/wind fields during the ablation season from 1970 to 2019 using correlation analysis. All data are detrended. Only significant correlations ($p < 0.05$) are shown. Vectors are composites of the correlations with horizontal wind components (zonal and meridional wind speed): a significant vector denotes either one of its components is significant. The geopotential height and wind field data are from the JRA55 dataset. SST data are from the HadISST dataset. Symbols are as follows: pink dot, Ts. Tuyuksu Glacier; pink inverted triangle, Kara-Batkak Glacier; pink cross, Abramov Glacier; blue square, Xiao Anglong Glacier.